Liquid-Crystalline Phase Development of a Mesogen-Jacketed Polymer—Application of Two-Dimensional Infrared Correlation Analysis†

Yi Shen,‡ Erqiang Chen,§ Chun Ye,§ Hailiang Zhang,§ Peiyi Wu,*,‡ Isao Noda,*,|| and Qifeng Zhou§

The Key Laboratory of Molecular Engineering of Polymers, Ministry of Education, Department of Macromolecular Science, Fudan University, Shanghai 200433, People's Republic of China, Department of Polymer Science and Engineering, College of Chemistry and Molecular Engineering, Peking University, Beijing 100871, People's Republic of China, and The Procter & Gamble Company, 8611 Beckett Road, West Chester, Ohio 45069

Received: November 1, 2004; In Final Form: January 21, 2005

Two-dimensional correlation spectroscopy has been applied to study PMPCS (poly{2,5-bis[(4-methoxyphenyl)-oxycarbonyl]styrene}), a representative example of mesogen-jacketed liquid crystalline polymers. With the precise analysis of a series of Fourier transform infrared (FTIR) spectra of PMPCS recorded at varied temperatures, a reasonable mechanism of the development of liquid crystalline (LC) phase is proposed. Before the phase transition, the conformational change of individual side chains occurs sooner than that of the backbone due to the larger motional freedom of the side chains. After the phase transition, however, the readjustment of still somewhat mobile backbone occurs before the ordered, rigid, and mutually interacting side chains. That is, phase transition leading to the LC phase formation brings in a new cooperative restriction of motions to the segments.

Introduction

Liquid-crystalline polymers (LCPs) have received considerable attention in recent years, because many high-performance materials can be prepared by processing LCPs in their mesomorphic state.[1−8] LCPs are available as both main-chain and side-chain LCPs, but their applications are often very different due to their properties determined by internally different molecular structures. Generally, the backbone of main-chain LCPs is so rigid that it can often be processed to high-strength and high-modulus material. On the other hand, compared with the side-chain LCPs, the requirement for processing such rigid main-chain LCPs is very rigorous.[9] Thus, it is always desired to find a way to contrive LCPs that possess excellent mechanical characteristics and can still be processed easily.

In 1987, Zhou et al. first proposed the concept of mesogen-jacketed liquid-crystalline polymers (MJLCPs).[10] MJLCPs are a kind of side-chain liquid crystalline polymers, in which the mesogen units are laterally attached to the polymer main chain with or without short spacers. Mesogens are aligned parallel to each other as well as to the main chain; thus, they form a more or less cylindrical "mesogen jacket" around the main chain.[10] Due to this unique structure, MJLCPs possess the advantages of both main-chain and side-chain LCPs. Therefore, MJLCPs have attracted great attention in recent years. [11−18]

Although much work have been published on this special class of polymers, a large part of the literature so far focused attention primarily on the synthesis of various kinds of the MJLCPs with the aim to improve the mechanical properties of MJLCPs.[11−13,17,18] The research work centering on the fundamental mechanistic understanding of MJLCP behavior, especially the structural changes of MJLCPs during the phase transition process, still remains limited. For example, Wen et al.[16] discussed the interaction between the molecular chains by Fourier transform (FT) IR, FT Raman, and NMR previously. However, the result in NMR was not well explained. As the types of MJLCPs continue to grow and become much more diverse, the current state of the apparent lack of understanding of the essential features of this class of materials can considerably limit further development and applications.

In this paper, we apply two-dimensional infrared (2D IR) correlation spectroscopy to address one of the essential questions: the mechanism of the liquid crystalline (LC) phase development. The material studied is poly{2,5-bis[(4-methoxyphenyl)oxycarbonyl]styrene} (PMPCS), a representative example of MJLCPs.

Two-dimensional (2D) IR correlation is a spectral analysis method originally proposed by Noda.[19−22] Due to its capability to identify the number and peak position of underlying bands not so apparent in a conventional one-dimensional (1D) spectrum,[23,24] 2D spectroscopy is often looked upon as a useful initial probing tool to aid in the analysis of complex IR spectra. Two-dimensional IR correlation analysis has received great attention for its another ability: it can discern the specific order of events taking place under the influence of a controlling physical variable, such as temperature, concentration, time and so on. Two-dimensional analysis can often simplify spectral features corresponding to various inter- and intramolecular interactions and elucidate the relationships between spectral elements.

Thus, with the application of 2D IR correlation spectroscopy, the mechanism of the LC phase development of PMPCS, which is closely related to the sequential order of changes in the

† Dedicated to Professor Gi Xue on the occasion of his 60th birthday.

* To whom correspondence should be addressed: e-mail peiyiwu@fudan.edu.cn (P.W.) or noda.i@pg.com (I.N.).

‡ Fudan University.

§ Peking University.

|| The Procter & Gamble Company.

10.1021/jp045014w CCC: $30.25
Published on Web 03/10/2005

SCHEME 1: Chemical Structure of PMPCS[a]

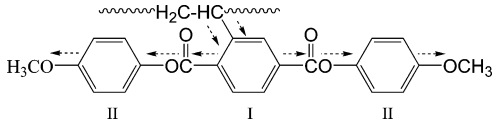

[a] Arrowheads indicate the sequence of changes in spectral intensities of the functionalities in PMPCS in the temperature range 140−220 °C.

molecular environment and conformations of various functional groups during the temperature elevation process, is probed. It appears that the cooperative restriction of motions to the segments is just opposite before and after the phase transition range of PMPCS.

Experimental Section

Materials. The polymer material studied is a representative mesogen-jacketed liquid crystal polymer, poly{2,5-bis[(4-methoxyphenyl)oxycarbonyl]styrene} (PMPCS). It has been supplied by the group of Qifeng Zhou[25−27] at Peking University (M_w = 25500). The chemical structure of PMPCS is shown in Scheme 1. The middle aromatic ring is simply called ring I hereafter, and the side aromatic rings are called ring II.

Measurements. All time-resolved FTIR spectra were collected on a Bruker-IFS-113V FTIR spectrometer with a resolution of 4 cm^{-1}, and 32 scans were accumulated to obtain an acceptable S/N ratio. The spectra were recorded in a variable-temperature cell between 80 and 220 °C with in increments of 10 °C. The wavenumber range recorded was 400−4000 cm^{-1}. Original spectra were baseline-corrected by use of Omnic 5.1 software.

FTIR spectra collected in the temperature range 80−220 °C were used to perform the 2D IR correlation analysis. The 2D contour maps were plotted by MATLAB software. The 1D spectra shown at the side and top of the 2D correlation maps are the average over the temperature range and are used as the reference. In the 2D contour maps, unshaded regions indicate positive correlation intensities, while shaded regions are for the negative ones.

Result and Discussion

A series of FTIR spectra of PMPCS in the temperature range 80−220 °C are shown in Figure 1a. For the sake of clarity, only 20 °C intervals are shown. Due to the importance of the CH stretching modes, carbonyl stretching modes, and the skeletal bands of aromatic ring, a close-up view of Figure 1a in the regions 3250−2700 and 1850−1450 cm^{-1} is plotted in Figure 1b. Tentative band assignments are listed in Table 1.[28−40,43] It is of particular note that the bands at 1508 and 1498 cm^{-1} are assigned to the skeleton vibration of ring II due to the disappearance of the skeleton vibration of ring I caused by the uniform substitutions in 2,4-positions.

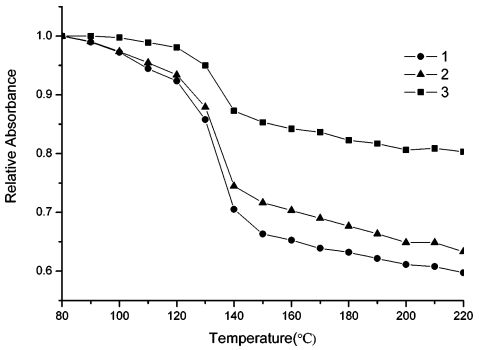

Figure 2. Temperature dependence of the relative absorbance of three typical bands centering around (1) 1732, (2) 2835, and (3) 3004 cm^{-1} in PMPCS.

TABLE 1: Tentative Assignment of the Spectral Bands[28−40,43]

peak position (cm^{-1})	assignment (tentative)
3080, 3004	ν_{ar}(CH) in the aromatic ring (ring I, disordered)
3032	ν_{ar}(CH) in the aromatic ring (ring II, ordered)
2985	ν_{as}(CH_3) of -OCH_3 (ordered)
2958	ν_{as}(CH_3) of -OCH_3 (disordered)
2935 (2942, 2925)	ν_{as}(CH_2) of -CH_2- (2942, disordered; 2925, relatively ordered)
2910	ν_{as}(CH_3) of -CH_2 (disordered)
2875, 2820	ν_s(CH_3) of -OCH_3 (ordered)
2835	ν_s(CH_2) of -CH_2- (disordered)
1732	$\nu_{C=O}$ of -COO- (disordered)
1508	skeleton vibration of aromatic ring (ring II, disordered)
1498	skeleton vibration of aromatic ring (ring II, ordered)

Confirmation of the Phase Transition Range. Figure 2 shows the temperature dependence of the relative absorbance of three typical bands of PMPCS centered around 3004, 2835, and 1732 cm^{-1}. It is noted that all the absorbance bands decreased with increasing temperature. The onset temperature of a significant decrease in the absorbance is about 120 °C, indicating the occurrence of a phase transition and the development of LC phase. After 160 °C, the values of the absorbance remained close to a constant value for each band at any given temperature. Thus, the phase transition range is determined to be from 120 °C to 160 °C, which accorded well with the result

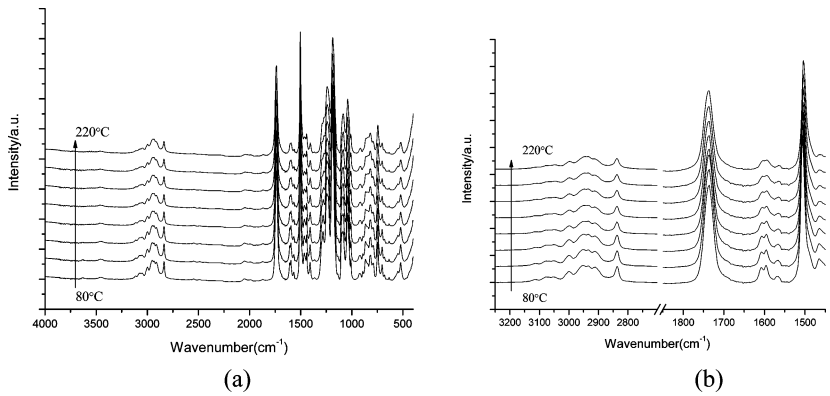

Figure 1. FTIR spectra of PMPCS (baseline-corrected): (a) in the range 4000−400 cm^{-1}; (b) in the range 3250−1450 cm^{-1}, with a break from 2700 to 1850 cm^{-1}.

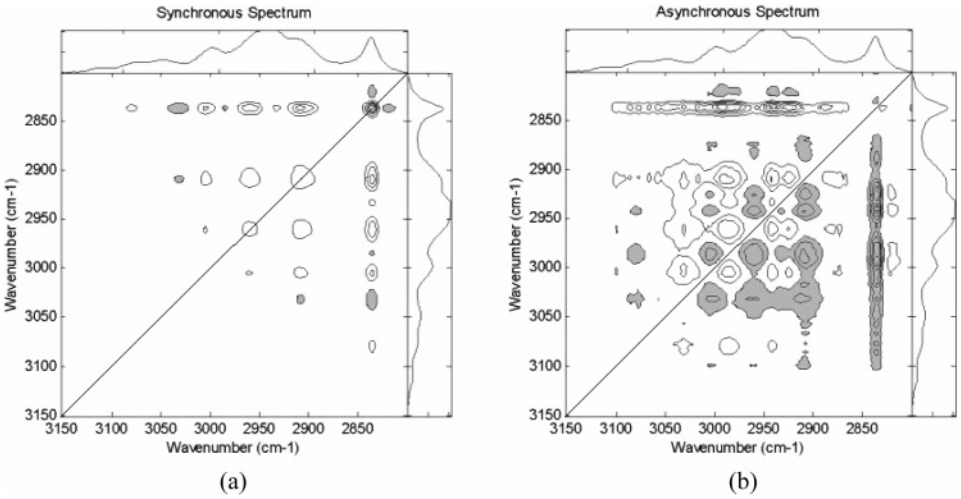

Figure 3. Two-dimensional (a) synchronous and (b) asynchronous correlation spectra of PMPCS in the 3150−2800 cm^{-1} region, in the temperature range 140−220 °C.

obtained from wide-angle X-ray diffraction experiment (WAXD; not shown here).[41]

The morphology of PMPCS film changed from the amorphous state to the LC state and then remained in the same LC state within the investigated temperature range, since the decomposition temperature of PMPCS is lower than its clear point. Here, it should be pointed out that the mesophase of PMPCS cannot be clearly identified either as the nematic phase or as the smectic phase, although in some literature, the PLM result suggested that the liquid crystal was probably in nematic form.[10,42]

Two-Dimensional Correlation Analysis. Given that the phase transition range is located between 120 °C and 160 °C, we separated the whole spectral data set of the investigated range into two connected ranges, 80−140 and 140−220 °C, and performed the 2D correlation analysis separately.

Two-Dimensional Analysis of Spectra in the Temperature Range 140−220 °C. Figure 3panels a and b, respectively, show the 2D synchronous and asynchronous contour maps of PMPCS in the CH stretching vibration range (3150−2800 cm^{-1}). In the 2D spectra, the positive and negative correlation intensities appear in the form of cross-peaks due to the fact that 2D correlation intensity is a function of two independent wavenumbers (the *x*-axis wavenumber ν_1 and the *y*-axis wavenumber ν_2).[24] In Figure 3a, three autopeaks (peaks located at diagonal positions, where $\nu_1 = \nu_2$) are found centering around 2835, 2910, and 2958 cm^{-1}, indicating that these bands changed intensities to a great extent under the thermal perturbation.[19] Eight positive cross-peaks at 2910/2835, 2935/2835, 2958/2835, 3004/2835, 3080/2835, 3004/2910, 3004/2958, and 2958/2910 cm^{-1} indicate that the intensities of these bands decreased together during the heating process, whereas the bands at 2820, 2985, and 3032 cm^{-1} shared negative 2D signals with the bands at 2835 and 2910 cm^{-1}, suggesting that the intensities of the former three bands increased during the observation interval. Compared with Figure 3a, the asynchronous spectrum in Figure 3b has many more cross-peaks, and the apparent features seem to be much more complex.

According to the so-called Noda's rule,[24] the appearance of a cross-peak $\Psi(\nu_1/\nu_2)$ in an asynchronous 2D correlation spectra indicates that the intensities of bands ν_1 and ν_2 vary out of phase with each other. The sign of an asynchronous cross-peak becomes positive if the intensity change at ν_1 occurs predominantly before ν_2 in the sequential order of the external variable. It becomes negative, on the other hand, if the change occurs after ν_2. This rule, however, is reversed if $\Phi(\nu_1/\nu_2) < 0$. On the basis of the above set of rules, the sequence of the band intensity changes corresponding to the coordinates of the cross-peak under the thermal perturbation can be easily summarized. The results are listed in Table 2. For example, the negative synchronous cross-peak Φ (2985/2835 cm^{-1}) and the positive asynchronous cross-peak Ψ (2985/2835 cm^{-1}) indicate that the intensity change of the band at 2835 cm^{-1} varied sooner (i.e., at a lower temperature) than that of the band at 2985 cm^{-1} in the temperature range 140−220 °C. The rest may also be deduced in an analogous fashion. Accordingly, by sorting out the set of such pairwise sequential relations in Table 2, one sees that the intensity change of the band at 2935 cm^{-1} (split into two subbands at 2925 and 2942 cm^{-1}) may be deduced to occur prior to any other bands, and the band at 2985 cm^{-1} changes intensity at the last stage.

TABLE 2: Summary of the Sequence of Band Intensity Changes under Thermal Perturbation in the Temperature Range 140−220 °C[a]

positive cross-peak	motion sequence	negative cross-peak	motion sequence
2875/2835	2835 → 2875	2942/2820	2942 → 2820
2925/2835	2925 → 2835	2925/2820	2925 → 2820
2935/2835	2935 → 2835	2835/2820	2835 → 2820
2942/2835	2942 → 2835	2985/2820	2820 → 2985
2958/2835	2958 → 2835	2910/2875	2910 → 2875
2985/2835	2835 → 2985	2958/2875	2958 → 2875
3032/2835	2835 → 3032	3004/2875	3004 → 2875
3080/2835	3080 → 2835	2958/2925	2925 → 2958
2925/2910	2925 → 2910	2958/2942	2942 → 2958
2942/2910	2942 → 2910	3004/2925	2925 → 3004
2985/2910	2910 → 2985	3004/2942	2942 → 3004
3032/2910	2910 → 3032	3080/2942	2942 → 3080
3080/2910	3080 → 2910	3004/2985	3004 → 2985
2942/2935	2942 → 2935	3080/2985	3080 → 2985
2985/2958	2958 → 2985	3080/3032	3080 → 3032
3032/2958	2958 → 3032		
3032/3004	3004 → 3032		

[a] All values are given as wavenumbers (i.e., in reciprocal centimeters).

We further sought for the relationship between the CH stretching vibration and the skeleton vibration of aromatic ring. The results are shown in Figure 4, in which the spectral range 3150−2800 cm^{-1} is correlated with the range 1550−1470 cm^{-1}. In the synchronous map (Figure 4a), the band at 1508 cm^{-1} shares cross-peaks with the bands at 2820, 2835, 2910, 2935,

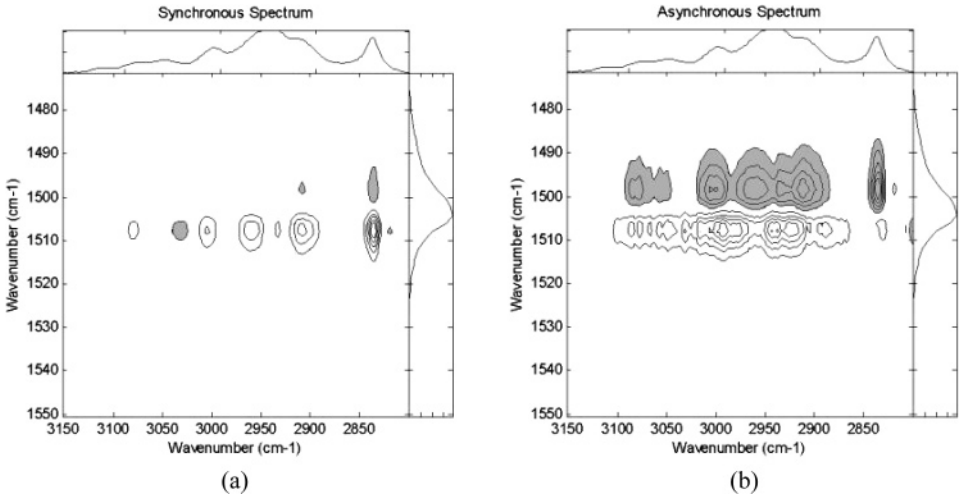

Figure 4. Two-dimensional (a) synchronous and (b) asynchronous correlation spectra of PMPCS in the 3150−2800 and 1550−1470 cm^{-1} regions, in the temperature range 140−220 °C.

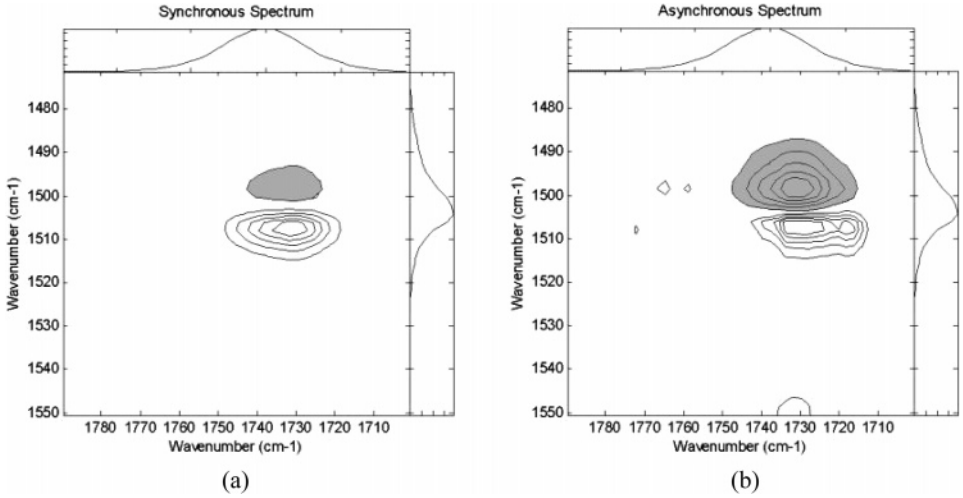

Figure 5. Two-dimensional (a) synchronous and (b) asynchronous correlation spectra of PMPCS in the 1790−1700 and 1550−1470 cm^{-1} regions, in the temperature range 140−220 °C.

2958, 3004, 3032, and 3080 cm^{-1}. Accordingly, the corresponding asynchronous cross-peaks in Figure 4b meant that the intensity change at 1508 cm^{-1} occurs prior to 2820 and 3032 cm^{-1} but later than 2835, 2910, 2935, 2958, 3004, and 3080 cm^{-1}. Additionally, two negative synchronous cross-peaks (2910/1498 and 2835/1498 cm^{-1}) and a row of the negative asynchronous cross-peaks at 1498 cm^{-1} (ν_2) suggested that the bands at 1508 and 1498 cm^{-1} had similar response behavior under thermal perturbation. A more detailed analysis (not shown here) illustrates that the 1508 cm^{-1} band has a slightly lower-temperature response compared to the 1498 cm^{-1} band.

The synchronous and asynchronous correlation signals of C═O stretching vibration (1790−1700 cm^{-1}) and skeleton vibration of the aromatic ring (1550−1470 cm^{-1}) are plotted in Figure 5, panels a and b, respectively. The cross-peaks located at 1732/1498 and 1732/1508 cm^{-1} lead to the conclusion that the intensity change at 1732 cm^{-1} occurs before 1508 and 1498 cm^{-1}.

In summary, we extracted the most essential bands located at 2935, 3080, 1732, 1508, 3032, and 2985 cm^{-1} to construct the final sequential order of spectral responses under thermal perturbation. These bands are important due to the fact that they represent the different functionalities in PMPCS. By sorting out the sequential relations mentioned above, the order of spectral intensity changes is 2935 cm^{-1} → 3080 cm^{-1} → 1732 cm^{-1} → 1508 cm^{-1} → 3032 cm^{-1} → 2985 cm^{-1}. These bands are in turn assigned to the $\nu_{as}(CH_2)$ of -CH_2- (in the backbone), ν_{ar}(CH) in aromatic ring (ring I), $\nu_{C=O}$ of -COO-, the skeleton vibration of aromatic ring (ring II), ν_{ar}(CH) in the aromatic ring (ring II), and $\nu_{as}(CH_3)$ of -OCH_3, respectively. That is, in the temperature range 140−220 °C, the backbone had an earlier (i.e., lower-temperature) response compared to the side chain of PMPCS. The sequence of changes is labeled by the arrowheads plotted in Scheme 1.

Two-Dimensional Analysis of Spectra in the Temperature Range 80−140 °C. Seven spectra of PMPCS in the temperature range 80−140 °C were used to perform the 2D correlation analysis. Two-dimensional spectra of CH stretching vibrations are shown in Figure 6. The spectral ranges in Figure 6 (3120−2800 cm^{-1}) and Figure 3 (3150−2800 cm^{-1}) are about the same, and there is a strong similarity between the positions of the cross-peaks in these figures. However, it is of particular note that the signs of the asynchronous cross-peaks in Figure 6b are opposite to those in Figure 3b. The result suggests that, in the temperature range 80−140 °C, the backbone of PMPCS had a delayed response to the controlling physical variable (temperature, in this work) compared with the side chain. Figures 7 and 8 provide good support for the conclusion. For example, the strong negative asynchronous cross-peak 2935/1508 cm^{-1} shown in Figure 7b illustrates that the intensity change at 1508

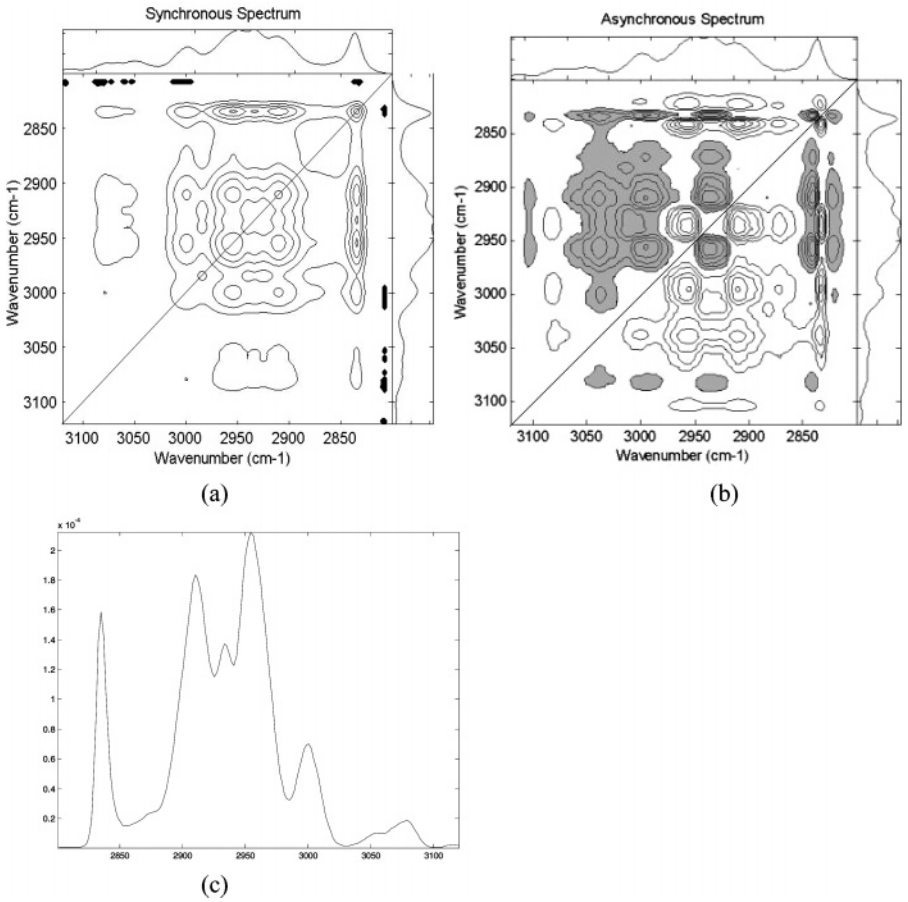

Figure 6. Two-dimensional (a) synchronous and (b) asynchronous correlation spectra of PMPCS in the 3120−2800 cm^{-1} region, in the temperature range 80−140 °C. (c) Power spectrum extracted along the diagonal line in panel a.

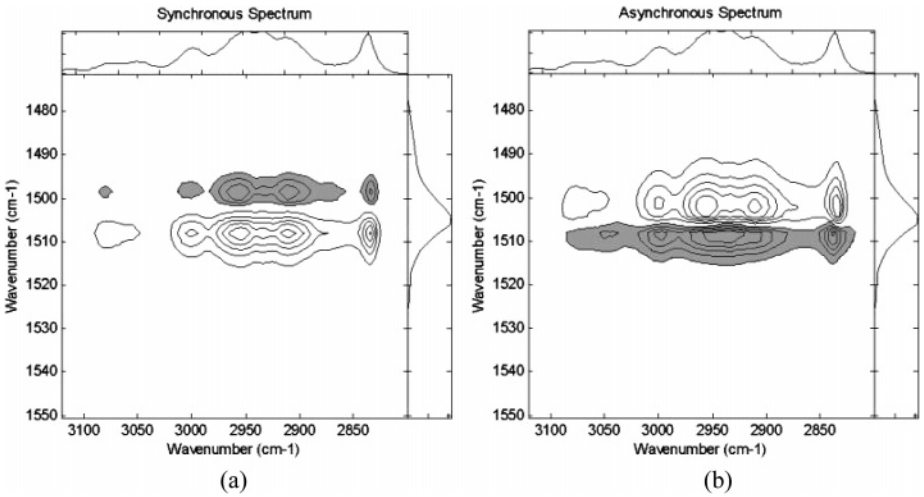

Figure 7. Two-dimensional (a) synchronous and (b) asynchronous correlation spectra of PMPCS in the 3120−2800 and 1550−1470 cm^{-1} regions, in the temperature range 80−140 °C.

cm^{-1} occurred before 2935 cm^{-1}. The cross-peak 1732/1508 cm^{-1} in Figure 8b indicates that ring II had an earlier (i.e., lower temperature) response compared to the functionality -COO-. As for the other cross-peaks, they just confirmed the similar sequential order.

It should be pointed out here that the circular features centering around 2875 and 2985 cm^{-1} at the diagonal line in Figure 6a are not autopeaks but troughs according to the corresponding power spectrum (Figure 6c). Also, the lack of 2D signals at 3032 cm^{-1}(ν_2) in Figure 6a suggests that, in the temperature range 80−140 °C, the intensity changes of the three bands at 2875, 2985, and 3032 cm^{-1} are very small.

Further Analysis. It is observed that the band at 2935 cm^{-1} is split into two subbands at 2942 and 2925 cm^{-1} in Figures 3b and 4b, whereas in Figures 6b and 7b, the intensity of the subband at 2925 cm^{-1} is very weak. That is, the subband at 2925 cm^{-1} gradually develops well after the phase transition range. A more detailed analysis shows that, in the temperature range 140−220 °C, the intensity change at 2942 cm^{-1} occurs before 2925 cm^{-1}, suggesting that after the phase transition,

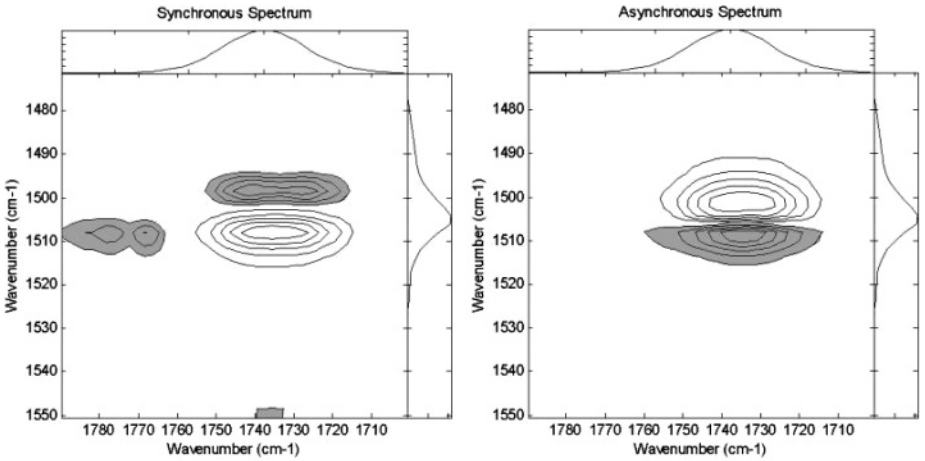

Figure 8. Two-dimensional (a) synchronous and (b) asynchronous correlation spectra of PMPCS in the 1790−1700 and 1550−1470 cm^{-1} regions in the temperature range 80−140 °C.

the overall band shape appears to shift to the lower wavenumber (2942 → 2925 cm^{-1}). The slight shift indicates that a more ordered conformational state is formed in PMPCS.[43] Another example is the pair of the bands at 1508 and 1498 cm^{-1}, in which 1508 cm^{-1} is assigned to the aromatic ring (ring II) in the disordered conformational state and 1498 cm^{-1} is attributed to the aromatic ring (ring II) in the ordered conformational state. In the temperature range 140−220 °C, the intensity change at 1508 cm^{-1} occurs before that at 1498 cm^{-1}, and the intensity of the band at 1508 cm^{-1} decreases whereas that of the band at 1498 cm^{-1} increases gradually. The spectral features indicate the LC phase development of PMPCS.

Mechanism of Development of the Liquid-Crystalline Phase. From the former analysis, it has become obvious that the sequential order of the changes in the backbone and side chain is just opposite in the temperature ranges 80−140 and 140−220 °C.

Before the phase transition, segments in the backbone of PMPCS cannot obtain enough energy to adjust the conformation. On the other hand, because the side chains are attached to the backbone individually without being connected to each other, the freedom of side chains is potentially larger than that of the backbone. Thus, the side chain responds sooner than the backbone to the temperature. However, the side chain is large and contains a rigid group in the middle. Thus, the extent of the motion is not expected to be very large. After the phase transition, the backbone obtains enough energy and changes its conformation more easily compared to the side chain due to its internal flexibility. To some extent, it has the same characteristics of main-chain LCPs. Meanwhile, in this temperature range, the rigid conjugated structure in side chain becomes the essential factor to block the side chain moving freely. Thus, the backbone is proposed to adjust its conformation first, followed by the side chain. Because ring I connects directly to the backbone, it attains easier motion compared with other groups in the side chain. An important role the side chain plays in PMPCS is that it takes advantage of its large and rigid characteristic to compel the backbone to orient to form the LC phase.

Nevertheless, both the backbone and side chain contribute to the development of the LC phase. With increasing temperature, the amorphous form of PMPCS is increasingly transformed to the mesomorphic form.

Conclusions

In this work, two-dimensional IR correlation analysis was used as a tool to study the mechanism of the LC phase development in PMPCS, a typical kind of mesogen-jacketed LCPs. The perturbation variable used for the 2D IR experiment was temperature.

The phase transition range 120−160 °C was examined according to the temperature dependence of the intensities at 1732, 2835, and 3004 cm^{-1}. Two-dimensional correlation analysis was performed on the temperature-dependent IR spectra to probe the sequential order of changes in the different functionalities of PMPCS in the temperature range 80−140 and 140−220 °C. The conclusions are as follows:

(i) Both the backbone and side chain contribute to the LC phase development, although the functional group responsible for the formation of liquid-crystalline phase is located only in the side chain.

(ii) In the temperature range 80−140 °C, the side chain responds at a lower temperature compared with the backbone because the side chains are attached to the backbone individually but not with each other, thus having larger freedom of motion.

(iii) In the temperature range 140−220 °C, since the backbone gains enough energy and the segments are internally flexible, the backbone varies at a lower temperature than the side chain. Consequently, the IR intensity of the ring I varies just after the backbone, then followed by the other functionalities in the side chain.

(iv) The earlier motion of the functionalities in disordered conformational state compared to those with ordered conformation under thermal perturbation probably explains the relative ease of development of LC phase in PMPCS.

Thus, a mechanism for the development of liquid crystalline phase is proposed. Before the phase transition, the conformational change of individual side chains occurs sooner than that of the backbone due to the larger freedom of the side chains. After the phase transition, however, the readjustment of still somewhat mobile backbone occurs before the ordered, rigid, and mutually interacting side chains. That is, phase transition leading to the LC phase formation brings in a new cooperative restriction of motions to the segments.

Acknowledgment. We gratefully acknowledge the financial support by the National Science Foundation of China (NSFC) (20425415, 20274010, 50103003, 20221402, 20134010, and

20025414), the "Qimingxing" Project (04QM1402) of Shanghai Municipal Science and Technology Commission, and the "Shuguang" Project (01SG05) of the Shanghai Municipal Education Commission and Shanghai Education Development Foundation.

References and Notes

(1) Garcia, M.; Eguiazabal, J. I.; Nazabal, J. *Polym. Composite* **2002**, *23*, 592.
(2) Liang, Y. C.; Isayev, A. I. *Polym. Eng. Sci.* **2002**, *42*, 994.
(3) Marty, J. D.; Mauzac, M.; Fournier, C.; Rico-Lattes, I.; Lattes, A. *Liq. Cryst.* **2002**, *29*, 529.
(4) Andreozzi, L.; Bagnoli, M.; Faetti, M.; Giordano, M. *Mol. Cryst. Liq. Cryst.* **2002**, *372*, 1.
(5) Chiezzi, L.; Fodor-Csorba, K.; Galli, G.; Gallot, B.; Pizzanelli, S.; Veracini, C. A. *Mol. Cryst. Liq. Cryst.* **2002**, *372*, 69.
(6) Liu, N.; Lin, J. P.; Chen, T.; Chen, J. D.; Zhou, D. F.; Li, L. *Polym. J.* **2001**, *33*, 898.
(7) Czarnecki, M. A.; Okretic, S.; Siesler, H. W. *Vib. Spectrosc.* **1998**, *18*, 17.
(8) Zebger, I.; Rutloh, M.; Hoffmann, U.; Stumpe, J.; Siesler, H. W.; Hvilsted, S. *J. Phys. Chem. A* **2002**, *106*, 3454.
(9) Zhao, Y. F.; et al. *Adv. Liq. Cryst. Poly. Supramol.* **2002**.
(10) Zhou, Q. F.; Li, H. M.; Feng, X. D. *Macromolecules* **1987**, *20*, 233.
(11) Gopalan, P.; Andruzzi, L.; Li, X. F.; et al. *Macromol. Chem. Phys.* **2002**, *203*, 1573.
(12) Tu, H. L.; Zhang, D.; Wan, X. H.; et al. *Macromol. Rapid Commun.* **1999**, *20*, 549.
(13) Pragliola, S.; Ober, C. K.; Mather, P. T.; et al. *Macromol. Chem. Phys.***1999**, *200*, 2338.
(14) Xu, G. Z.; Hou, J. N.; Zhu, S. N.; Yang, X. Z.; Xu, M.; Zhou, Q. F. *Polymer* **1994**, *35*, 5441.
(15) Xu, G. Z.; Wu, W.; Shen, D. Y.; Hou, J. N.; Zhang, S. F.; Xu, M.; Zhou, Q. F. *Polymer* **1993**, *34*, 1818.
(16) Wen, Z. Q.; Shen, D. Y.; Zhou, Q. F.; Zhu, X. L. *Acta Polym. Sin.* **1991**, *4*, 430.
(17) Gopalan, P.; Pragliola, S.; Ober, C.; et al. *Abstr. Pap. Am. Chem. S.* **1999**, *218*, 356.
(18) Zhou, Q. F.; Wan, X. H.; Zhang, D.; et al. *ACS Symp. Ser.* **1996**, *632*, 344.
(19) Noda, I. *Appl. Spectrosc.* **1993**, *47*, 1329.
(20) Noda, I. *Bull. Am. Phys. Soc.***1986**, *31*, 520.
(21) Noda, I. *J. Am. Chem. Soc.* **1989**, *111*, 8116.
(22) Noda, I. *Appl. Spectrosc.* 1**990**, *44*, 550.
(23) Elmore, D. L.; Dluhy, R. A. *Colloids Surf. A: Physicochem. Eng.* **2000**, *171*, 225.
(24) Noda, I.; Dowrey, A. E.; Marcott, C.; Story, G. M.; Ozaki, Y. *Appl. Spectrosc.* **2000**, *54*, 236A.
(25) Yin, X. Y.; Ye, C.; Ma, X.; et al. *J. Am. Chem. Soc.* **2003**, *125*, 6854.
(26) Zheng, R. Q.; Chen, E. Q.; Cheng, S. Z. D.; et al. *Macromolecules* **2000**, *33*, 5159.
(27) Li, C. Y.; Tenneti, K. K.; Zhang, D.; et al. *Macromolecules* **2004**, *37*, 2854.
(28) Sheppard, N.; Simpson, D. M. *Q. Rev.* **1953**, *7*, 19.
(29) Henbest, H. B.; et al. *J. Chem. Soc.* **1957**, 1462.
(30) Dalton, F.; et al. *J. Chem. Soc.* **1960**, 2927.
(31) Bernstein, H. J. *Spectrochim. Acta* **1962**, *18*, 161.
(32) Katritzky, A. R. *J. Chem. Soc.* **1958**, 4162.
(33) Katritzky, A. R.; Simmons, P. *J. Chem. Soc.* **1959**, 2058.
(34) Katritzky, A. R.; Lagowski, J. M. *J. Chem. Soc.* **1958**, 4155.
(35) Katritzky, A. R.; Jones, R. A. *J. Chem. Soc.* **1959**, 3670.
(36) Katritzky, A. R. *J. Chem. Soc.* **1959**, 2051.
(37) Mckean, D. C.; et al. *Spectrochim. Acta* **1973**, *29A*, 1037.
(38) Forel, M. T.; et al. *J. Opt. Soc. Am.* **1960**, *50*, 1228.
(39) Shimanko, N. A.; Shishkina, M. V. *Infrared and U. V. Absorption Spectra of Aromatic Esters*; Nauka: Moscow, 1987.
(40) Socrates, G. *Infrared Characteristic Group Frequencies-Tables and Charts*, 2nd ed.
(41) Ye, C.; Zhang, H. L.; Huang, Y.; et al. *Macromolecules* **2004**, *37*, 7188.
(42) Zhang, H.; Yu, Z.; Wan, X.; Zhou, Q. F.; Woo, E. M. *Polymer* **2002**, *43*, 2357.
(43) Synder, R. G.; Hsu, S. L.; Krimm, S. *Spectrochim. Acta* **1978**, *34A*, 395.